

Synchrotron radiation studies of mass-selected Fe nanoclusters deposited *in situ*

C. Binns^{1,a}, S.H. Baker¹, M.J. Maher¹, S.C. Thornton¹, S. Louch¹, S.S. Dhesi², and N.B. Brookes²¹ Department of Physics and Astronomy, University of Leicester, Leicester LE1 7RH, UK² ESRF, BP 220, F-38043 Grenoble Cedex, France

Received 14 December 2000

Abstract. A portable UHV-compatible gas aggregation cluster source, capable of depositing clean mass-selected nanoclusters *in situ*, has been used at synchrotron radiation facilities to study the magnetic behaviour of exposed and Co-coated Fe clusters in the size range 250 to 540 atoms. X-ray magnetic circular dichroism (XMCD) studies of isolated and exposed 250-atom clusters show a 10% enhancement in the spin magnetic moment and a 75% enhancement in the orbital magnetic moment relative to bulk Fe. The spin moment monotonically approaches the bulk value with increasing cluster size but the orbital moment does not measurably decay till the cluster size is above ~ 400 atoms. The total magnetic moments for the supported particles though higher than the bulk value are less than those measured in free clusters. Coating the deposited particles with Co *in situ* increases the spin moment by a further 10% producing a total moment per atom close to the free cluster value. At low coverages the deposited clusters are superparamagnetic at temperatures above 10 K but a magnetic remanence at higher temperature emerges as the cluster density increases and for cluster films with a thickness greater than 50 Å (*i.e.* 2-3 layers of clusters) the remanence becomes greater than that of an Fe film of the same thickness produced by a conventional deposition source. Thick cluster-assembled film show a strong in-plane anisotropy.

PACS. 75.50.Tt Fine-particle systems; nanocrystalline materials

1 Introduction

Nanoscale magnetic particles with sizes below 5 nm are attracting a great deal of attention due to both, a fundamental interest in mesoscopic physics, and their potential utility in industrial materials. The reduced average atomic co-ordination and resulting narrowing of the valence d bands leads to enhanced (orbital and spin) magnetic moments [1,2]. Additional novel effects arise from the nanoscale confinement of the valence electron gas. Films assembled from clusters and non-magnetic conducting or insulating matrices show giant magnetoresistance (GMR) [3,4] and tunnel magneto-resistance (TMR) [5] phenomena.

Here we report a study of the evolution of the magnetic behaviour of films assembled from Fe clusters as a function of cluster size in the case of isolated clusters and as a function of density on the surface from the dilute limit through to thick films. All the measurements on exposed particles were carried out by depositing clusters *in situ* using a UHV-compatible gas aggregation source equipped with a quadrupole mass filter operating at masses up to 32000 amu [6]. Some of the cluster films were coated with Co *in situ* to determine the effect of a magnetic embedding matrix.

2 Morphology of cluster assembled films

Scanning Tunnelling Microscope (STM) images of unfiltered Fe clusters deposited *in situ* onto Si(111)-(7×7) surfaces at 300 K are shown for two different doses in Figs. 1a and 1b. The kinetic energy acquired by the particles in the free jet expansion is estimated to be of the order of 0.1 eV per atom so the impact on the surface is well within the “soft landing” regime. There is no evidence for diffusion, which would be revealed by a tendency for the clusters to agglomerate into larger structures or line up along atomic steps in the substrate surface. Even at high coverage where the beam impinges on adsorbed clusters, they do not coalesce and the film retains its granular structure. Closer inspection shows that the particles are faceted and they tend to attach to others along the facets. The cluster height distribution of the film in Fig. 1a is shown in Fig. 1c and displays a log-normal shape with a most probable height of 2.2 nm. Also shown in Fig. 1c is a shifted distribution obtained with the mass filter. The average height to width ratio of the clusters is 0.7. The STM study was carried out for Fe clusters on Si(111) whereas the magnetic measurements were on Fe clusters on highly oriented pyrolytic graphite (HOPG). It is clear from the magnetic measurements presented below that, at low coverages, the deposited films consist of isolated

^a e-mail: cb12@le.ac.uk

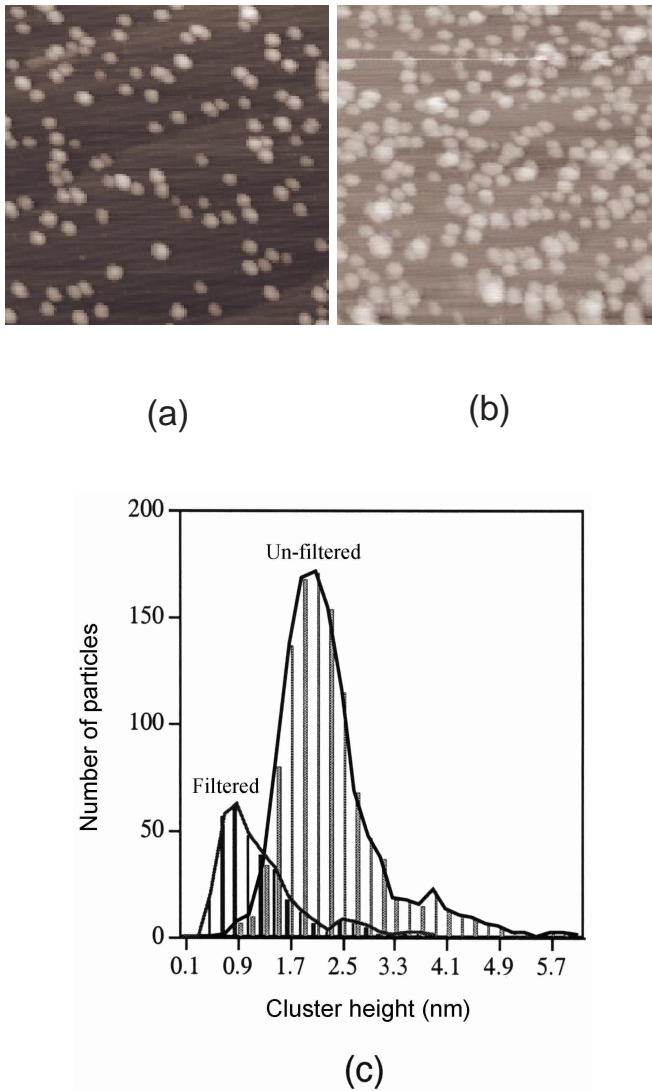


Fig. 1. Morphology of exposed Fe clusters on Si(111). (a) and (b) STM images (100×100 nm) of un-filtered cluster depositions at different coverages. (c) Height distribution of un-filtered and mass-filtered clusters.

particles with the same size as the quadrupole filter setting so we assume that the morphology on graphite is similar to that shown in Fig. 1.

3 Magnetic behaviour of isolated clusters on HOPG

Orbital (m_L) and spin (m_S) magnetic moments were measured as a function of cluster size using X-Ray Magnetic Circular Dichroism (XMCD) on beamline ID12B at the ESRF, Grenoble. A series of films composed of clusters with sizes 250, 300, 386, 450 and 540 ± 25 atoms was deposited onto HOPG up to an equivalent thickness of 0.6 Å, that is, about 3% coverage. The sample temperature

during deposition was maintained at 10 K. Magnetisation ($M - H$) curves obtained from the variation of the FeL₃ absorption edge as a function of coverage showed that at 40 K the particles were superparamagnetic and the “magnetic size” obtained by fitting Langevin functions to the curves agreed with the mass filter setting for all samples. This verifies that the particles remain isolated and do not agglomerate. The blocking temperature was below 10 K for all particle sizes.

Fig. 2 shows the size-dependent variation in the orbital and spin moments obtained by applying the magneto-optical sum rules [7] to the dichroism spectra recorded with the applied magnetic field, \mathbf{M} at $\theta = 0^\circ$ and at $\theta = 55^\circ$ (the “magic” angle) relative to the surface normal. In this experiment the direction of the X-ray beam and thus the photon angular momentum was always parallel or anti-parallel to \mathbf{M} . For the smallest clusters, there is an 75% increase in m_L relative to the bulk value that decreases towards the bulk with increasing size. The value of m_L does not show a significant variation with angle indicating that the magneto-crystalline anisotropy has similar values in-plane and out-of-plane [8]. Unlike the spin moment, m_L does not continue to increase below 400 atoms so that the orbital to spin ratio decreases in the smallest clusters. This is discussed below. Even at the lowest temperatures attainable (6 K), the remanence, measured by saturating the sample and recording the L₃ edge intensity at zero field, is small and isotropic for the isolated cluster films over the size range investigated. From its dependence on temperature we estimate that the anisotropy constant in the clusters is an order of magnitude greater than the bulk [9]. This is attributable to the enhanced orbital moment.

The spin sum rule contains the dipole moment, m_T , given by the expectation value of the intra-atomic dipole operator, $\langle T_Z \rangle$. This term has an angular average of zero and will also vanish for measurements on polycrystalline films or with data recorded at the magic angle for crystalline samples. The spin sum rule shows a variation with angle indicating that the clusters do not have a random distribution of crystal axes. We propose the most likely arrangement is that there is a common z -axis perpendicular to the surface for all particles and that the $x - y$ axes have a circular symmetry about the surface normal corresponding to the symmetry of the graphite surface. In this case the magic angle analysis is still valid and applying the sum rules to the XMCD spectra measured at $\theta = 55^\circ$ reveals the pure spin moment. In the 250 atom clusters this is enhanced by $\sim 10\%$ relative to the bulk value.

The increase in both m_L and m_S contributions to the magnetic moment can be ascribed to the high proportion of surface atoms with a low co-ordination. It is notable however that the ratio m_L/m_S is significantly lowered in the smallest clusters. As the cluster size is reduced, as well as an increasing proportion of atoms at the surface, there is also an increasing proportion influenced by the crystalline field at the cluster/substrate interface that will act to reduce m_L . We propose that this effect starts to dominate at sizes below 250 atoms.

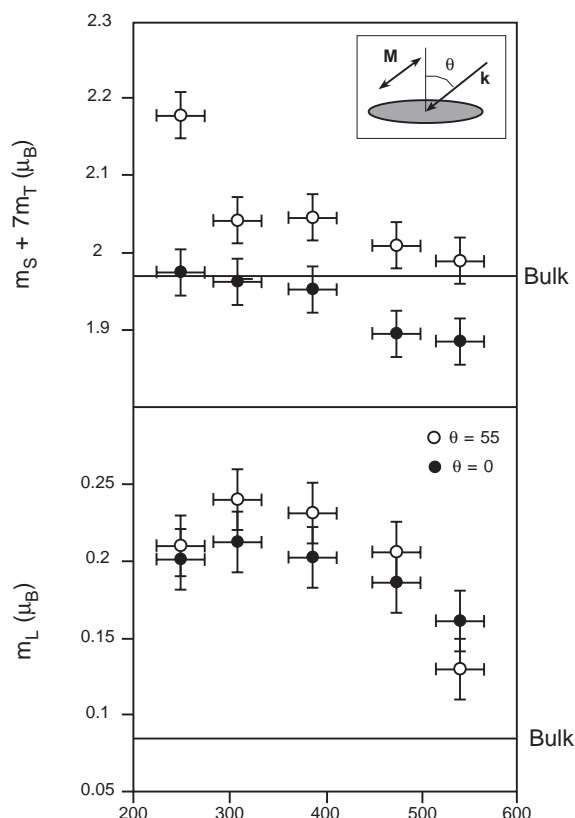


Fig. 2. Orbital and spin magnetic moments measured by XMCD for two different angles, θ , of the applied field and photon angular momentum relative to the surface normal. The pure spin moment is the value at $\theta = 55^\circ$. For $N = 250$, m_L , and m_S are enhanced by 75% and 10% respectively relative to the bulk. The inset shows the geometry of the measurement.

4 Magnetic behaviour of Co-coated clusters

Three of the exposed cluster assemblies, with sizes 250, 386 and 540 atoms, were coated *in situ* with a Co film of thickness 10 Å. This required that the sample was warmed to room temperature in order to transfer it into a preparation chamber. The orbital and spin magnetic moments in the exposed clusters were re-measured at room temperatures before coating to check that the cluster assembly had not agglomerated. No change of the orbital and spin moments could be detected within the experimental uncertainty verifying that the clusters remained isolated. Previous studies have shown [10] that the Co film is islanded with some of the islands containing embedded clusters. Since XMCD measures the dichroism at an absorption edge, the magnetic moments can be obtained for the Fe clusters separately from the matrix.

The Co coating produces a 10% increase in the spin moment relative to the exposed cluster value but no significant change in the orbital moment. A large increase in the Fe spin moment is observed in Fe–Co alloys and within a rigid band model is ascribed to an increase in the majority spin band population by electrons from the Co [11]. In this case there isn't a well mixed alloy as we know that

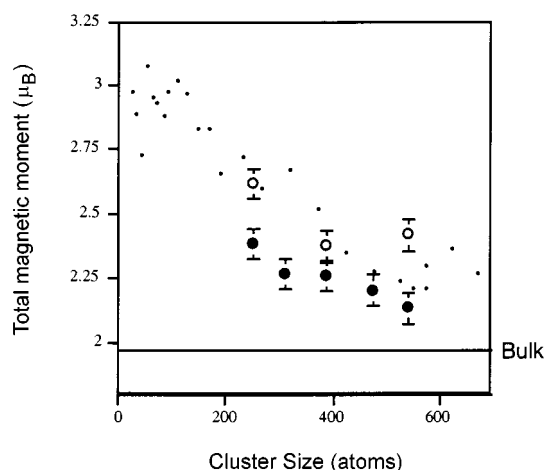


Fig. 3. Total magnetic moment in Fe clusters as a function of size for exposed clusters supported on HOPG (filled circles), Co-coated clusters on HOPG (open circles), and free clusters [1] (dots).

the Fe remains as particles within the matrix although there may be alloying at the interface [10]. In addition, no significant change is observed in the total FeL-edge X-ray absorption (“white line”) intensity indicating that there is no significant change in the number of Fermi level d -band holes in the Fe. This is consistent with an increase in the spin moment resulting from an increase in the Fe valence band exchange splitting produced by the interaction with the Co matrix. Interestingly, the anisotropy in the $m_S + 7m_T$ term is much less in the coated clusters than observed for the exposed particles (Fig. 2) indicating that the m_T contribution is significantly reduced to a value characteristic of a bulk sample. The lack of change in the orbital moment before and after coating is surprising since it would be expected to decrease if the Fe/vacuum interface is replaced by Fe/Co. The result could be due to a compensating increase in m_L arising, *via* the spin-orbit interaction, from the increased spin. Figure 3 shows the total moment (orbital + spin) for the exposed clusters and Co coated clusters. The results are compared to the total magnetic moments in free Fe clusters measured by their deflection in a gradient magnetic field [1].

5 Magnetic behaviour of exposed clusters as a function of density

Previous studies using XMCD have shown that the orbital and spin moments tend to the bulk values when clusters are assembled with a sufficient density that they come into contact [12]. Here we report magnetic linear (circular) dichroism in the angular distribution (ML(C)DAD) of photoelectrons emitted from the Fe3*p* core level. The technique measures the dichroism in the photoemission spectrum in response to reversing the alignment between the in-plane sample magnetisation and the linear polarisation of the XUV light (MLDAD [13]) or between

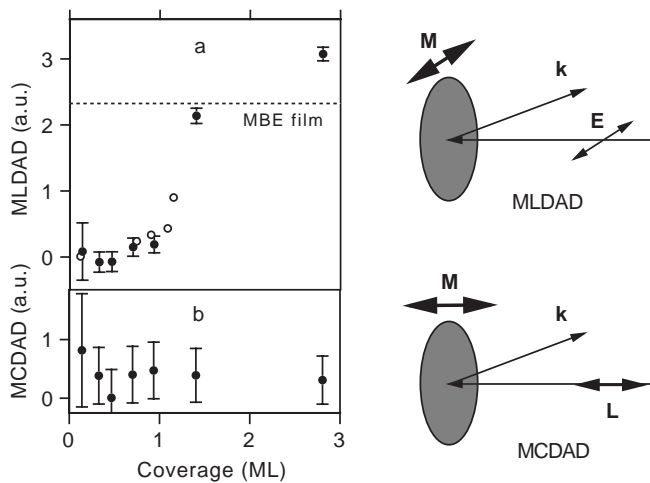


Fig. 4. (a) MLDAD signal (in-plane remanence) and (b) MCDAD signal (out-of-plane remanence) of Fe cluster films as a function of coverage in cluster monolayers measured at 40 K. The open circles are for clusters deposited on HOPG and the filled circles are for deposits on polycrystalline Cu. The remanence of 60 Å thick MBE layer is shown for comparison.

the out-of-plane sample magnetisation and angular momentum of circularly polarised light (MCDAD [14]). Since photoemission spectra must be collected in zero field, the technique only measures remanence but it is surface sensitive and capable of measuring sub-monolayer quantities of material. The two geometries are shown in Fig. 4 and using beamline 5D on the SRS, Daresbury, it is possible to select light with linear, or either helicity of circular polarisation and thus combine them in a single experiment. This enables the comparison of in-plane and out-of-plane remanent magnetisation.

Fig. 4 shows the development with density of the remanence at 40 K of un-filtered cluster films deposited on Cu and HOPG substrates. At low coverages, when the clusters are isolated, the samples are superparamagnetic at 40 K and show no remanent magnetisation. As the coverage increases and the clusters begin to interact a remanence at 40 K develops in-plane but no remanent component is observed out-of-plane at any coverage. Thus the isotropic

magnetisation for the isolated clusters is replaced by a strong in-plane anisotropy of the dense interacting assembly. We ascribe this to the shape anisotropy of the overall film. It can be seen that the remanence in a 60 Å thick cluster film exceeds that of an MBE Fe film of the same thickness.

References

1. I.M.L. Billas, J.A. Becker, A. Châtelain, W.A. de Heer, *Phys. Rev. Lett.* **71**, 4067 (1993).
2. D.C. Douglass, A.J. Cox, J.P. Bucher, L.A. Bloomfield, *Phys. Rev. B* **47**, 4067 (1993).
3. A.E. Berkowitz, J.R. Mitchell, M.J. Carey, A.P. Young, S. Zhang, F.E. Spada, F.T. Parker, A. Hutten, G. Thomas, *Phys. Rev. Lett.* **68**, 3745 (1992).
4. J.Q. Xiao, J.S. Jiang, C.L. Chien, *Phys. Rev. Lett.* **68**, 3749 (1992).
5. S. Mitani, H. Fujimori, K. Takanashi, K. Yakushiji, J.-G. Ha, S. Takahashi, S. Maekawa, S. Ohnuma, N. Kobayashi, T. Masumoto, M. Ohnuma, K. Hono, *J. Mag. Magn. Mater.* **198-199**, 179 (1999).
6. S.H. Baker, S.C. Thornton, K.W. Edmonds, M.J. Maher, C. Norris, C. Binns, *Rev. Sci. Instr.* **71**, 3178 (2000).
7. C.T. Chen, Y.U. Idzerda, H.-J. Lin, N.V. Smith, G. Meigs, E. Chaban, G.H. Ho, E. Pellegrin, F. Sette, *Phys. Rev. Lett.* **75**, 152 (1995).
8. D. Weller, J. Stöhr, R. Nakajima, A. Carl, M.G. Samant, C. Chappert, R. Mégy, P. Beauvillain, P. Veillet, G. Held, *Phys. Rev. Lett.* **75**, 3752 (1995).
9. K.W. Edmonds, C. Binns, S.H. Baker, M.J. Maher, S.C. Thornton, O. Tjernberg, N.B. Brookes, *J. Magn. Magn. Mater.* **231**, 113 (2001).
10. K.W. Edmonds, C. Binns, S.H. Baker, M.J. Maher, S.C. Thornton, O. Tjernberg, N.B. Brookes, *J. Mag. Magn. Mater.* **220**, 25 (2000).
11. P. Söderlind, O. Eriksson, B. Johansson, R.C. Albers, A.M. Boring, *Phys. Rev. B* **45**, 12911 (1992).
12. K.W. Edmonds, C. Binns, S.H. Baker, S.C. Thornton, C. Norris, J.B. Geodkoop, M. Finazzi, N.B. Brookes, *Phys. Rev. B* **60**, 472 (1999).
13. G. Panaccione, F. Sirotti, G. Rossi, *Sol. St. Commun.* **113**, 373 (2000).
14. G. van der Laan, *Phys. Rev. B* **51**, 240 (1995).